Powder Technology 324 (2018) 85–94

Contents lists available at ScienceDirect

Powder Technology

journal homepage: www.elsevier.com/locate/powtec

Evaluation of the mechanical properties of compacted paraffin powders. Effect of formulation

K. Dunchych [a,*], C. Loisel [b], A. Arhaliass [a], O. Gonçalves [a], J. Legrand [a], M. Pouliquen [c], S. Saint-Jalmes [c]

[a] Université de Nantes, - GEPEA UMR CNRS 6144, CRTT, boulevard de l'Université, 44600 Saint-Nazaire cedex, France
[b] ONIRIS, CS 82225, 44322 Nantes, France
[c] Denis et Fils, RN149 Recouvrance, 44190 Gétigné, France

ARTICLE INFO

Article history:
Received 1 June 2017
Received in revised form 12 September 2017
Accepted 9 October 2017
Available online 18 October 2017

Keywords:
Mechanical properties
Powder compressibility
Paraffin
Sustainability

ABSTRACT

The mechanical characteristics of a paraffin–vegetable oil material and the compressive behavior of the powder stemming from this material were used to estimate the resistance of the compressed samples. The compressive behavior of powders under the low pressure range (1–2 MPa) applied in the candle industry was investigated in order to predict the tensile strength of the compressed samples. Compressive behavior was evaluated under lab conditions similar to those practiced in the candle industry. Compressive behavior of the powders, which represents the resistance of the particles to rearrangement during the packing step, K_p (30.98 ± 1.20 kPa of the mixture M1), was positively correlated to tensile strength of the compressed samples, σ_t (175.46 ± 3.61 kPa of mixture M1). Tensile strength of the compacts was also related to the mechanical properties of the raw material: high tensile strength was linked to low ductility (γ_{MR}), high mechanical strength (R_{MR}) and high Young's modulus (E) of the material. Formulation—particularly the presence of a lubricant of mineral (0.52%) and vegetable (44.1%) origin in mixture M5—was found to strongly influence the mechanical properties of the compressed samples ($\sigma_t = 115.52 \pm 2.42$ kPa).

1. Introduction

The paraffin wax obtained from refining oil finds a wide range of applications in industry, medicine, and food, and is the main material used in compression-based candle manufacture. However, despite being in widespread use, the behavior of paraffin as a powder in compression has never yet been studied. Furthermore, research into alternative renewable materials of vegetable origin is thriving as the candle market looks for more sustainable sources. Several patents [1–3] state that the combination of alternative materials with paraffin wax has to meet the physical characteristics required, including controlled melting points, high malleability, low fragility, and high chemical stability. Vegetable oils of different origins (e.g. palm oil, rapeseed oil and olive oil) are candidates for mixing with paraffin, and the use of vegetable oils derived from vegetable waste is also described in certain patents [4]. In order to incorporate alternative materials in the candle, one has to verify their compatibility with a complex mechanical process, i.e. compression, to guarantee the quality of the final candle product.

The compression process is widely used in many industrial sectors, from pharmacy and metallurgy to cosmetics and foods. The success of the compression is related to the mechanical properties of the material [5–6] and of the powder bed, i.e. the ability of the powder to decrease in volume under pressure (compressibility) [7–11] and form a cohesive compact by densification (compactibility) [12–13], the transmission of forces through the powder volume [14–15], the mechanism involved in the cohesion of the tablet (solid bridges, forces of attraction, entanglements) [16–17], and inter-particle/wall friction during the compression [18–20]. All these parameters play an important role in the formation of a cohesive compressed sample.

The mechanical properties of the materials themselves, such as the ductile or brittle character of the material and its hardness/softness characterized by Young's modulus [21–26], also have to be taken into account. These parameters depend on the nature of the forces involved and the structure and purity of the material.

The behavior of the powder in compression is critical in the formation of the compressed sample. During compression, with the increase of the pressure, the powder undergoes intensive densification and the powder particles move together to generate cohesive forces [17,19,27]. Many studies have focused on the relationship between relative density of the powder and compaction pressure, considered as defining the compressibility of a material, and several models have been developed and modified to characterize the compressibility of powders [7–11,28]. When compression starts, the particles rearrange themselves by sliding and rotating to form a denser stack, thus

* Corresponding author.
E-mail address: kateryna.dunchych@univ-nantes.fr (K. Dunchych).

https://doi.org/10.1016/j.powtec.2017.10.029
0032-5910/

increasing the number of connection points between the particles [7–8,10–11]. With the increase in pressure, at the end of the packing step the particles cannot slide further and undergo deformations according to their mechanical characteristics [7–8,17,29–33]. The specific energy required during compression is related to the densification of the powder and depends mainly on pressure range and the physical properties of the material [34–36].

The tensile (or breaking) strength of compressed samples depends on the nature and intensity of the inter-particle bonds, and the contact surface between the particles. Comparisons of various materials are generally based on destructive tests [37–42]. Many studies have been carried out to understand the mechanisms of rupture of the compressed samples and to define the influence of various parameters on material strength. Several studies have investigated the relationship between tensile strength and the properties of the compressed samples, including compaction behavior, porosity, particle size, and particle shape [43–50]. Concerning the shape and surface of the grains, the more the grains are rough and irregularly shaped, the stronger the forces of inter-particle friction, which promotes the formation of solid bridges and improves the strength of the compressed samples [43–44,49].

Another factor contributing to the mechanical strength of the compressed sample is the presence of lubricant. The role of lubricants used in the manufacture of pharmaceutical tablets is to reduce the friction of the matrix walls and avoid powder sticking to the punches, and to improve the transmission of pressures in the volume of the powder bed by reducing the friction between the particles [51–55]. Although these parameters can improve the compression characteristics, they can also have negative effects on the quality of the grains, and especially on the mechanical strength of the samples [56–61].

The objective of this study was to provide a thorough understanding of the formation of a cohesive compacted sample from paraffin/vegetable substitute powders, and to define the predominant factors that explain the tensile strength of the compressed samples. The study was performed in three steps: (i) study of the mechanical characteristics of the material (deformation capacity and mechanical strength of the material, Young's modulus); (ii) study of the formation of the compressed samples (the compressive behavior of the powders) and energy requirements; (iii) determination of the tensile strength of the compressed samples. Particular emphasis was placed on the step of packing under low pressure, where rearrangement of the particles is the dominant behavior. The influence of formulation (paraffin and vegetable substitute) and presence of lubricant in the formulation was studied in the three characterization steps.

The main purpose of this study was to produce compressed samples with the highest tensile strength while working in low pressure ranges (up to 2 MPa) used in candle manufacture.

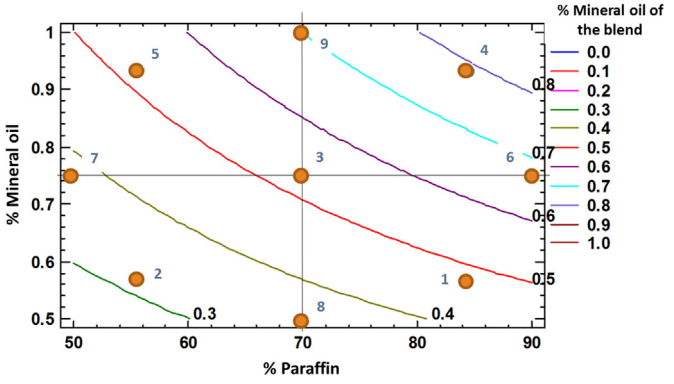

Fig. 1. Experimental area of the second-order central composite design.

Table 1
Composition and characteristics of the five mixtures. Mean ± standard deviation.

Mixture	Composition			Melting point (°C)	Density (g/cm^3)
	% Paraffin (fully and semi)	% Vegetable oil	% Mineral oil of the blend		
M1	84.1	15.9	0.48	54.27 ± 0.23	0.92 ± 0.002
M2	55.9	44.1	0.32	49.43 ± 0.41	0.93 ± 0.002
M3	70	30	0.53	48.10 ± 0.15	0.92 ± 0.002
M4	84.1	15.9	0.78	52.45 ± 0.32	0.91 ± 0.001
M5	55.9	44.1	0.52	49.56 ± 0.67	0.93 ± 0.003

2. Materials and methods

2.1. Materials

Two types of paraffin and a transformed vegetable oil (stearin) were used: fully-refined paraffin containing 0.5% mineral oil (defined by standard method ASTM D 721) and semi-refined paraffin containing 1%. The paraffin predominantly contains linear hydrocarbons with a carbon chain distribution of C18–C40 (based on GC analysis on an Agilent 7820A system, Santa-Clara, CA, USA). The stearin is composed of free fatty acids, i.e. 50% palmitic acid and 50% stearic acid (based on GC analysis on an Agilent 7820A system, Santa-Clara, CA, USA). Five mixtures (M1-M5) formulated by the experimental second-order central composite design realized by Statgraphics Centurion 17.1.06 (Graphics Software System, STCC, Inc. USA.) were used in our study, as illustrated in Fig. 1.

The composition and characteristics of the blends are given in Table 1. Melting point of the mixtures varied between 48 and 54 °C

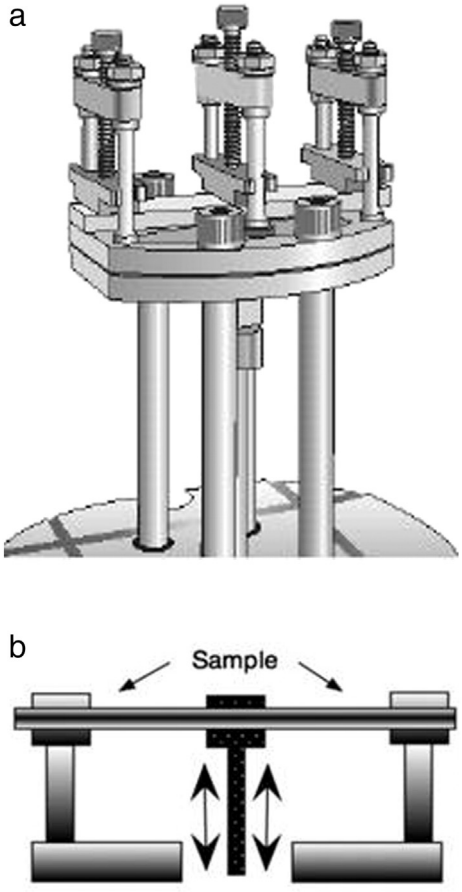

Fig. 2. a) 3-point bending dual cantilever device (TA Instruments Q800 DMA); b) Scheme of dual cantilever device used for rupture test.

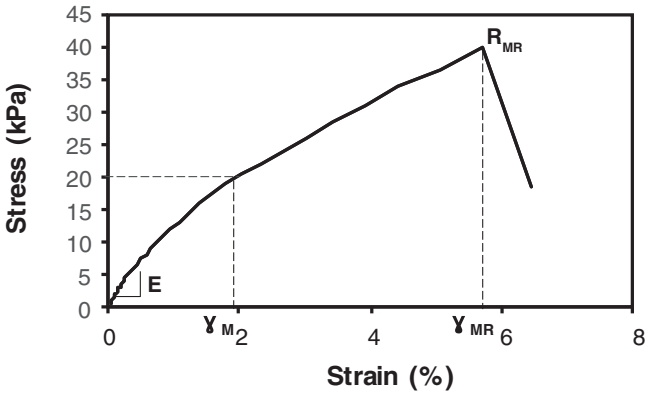

Fig. 3. Typical stress - strain curve of the material.

(measured by differential scanning calorimetry (DSC) on a TA Instruments Q100 V9.9 system, New Castle, DE, USA). The true density, ρ_s, at 25 °C (measured with an AccuPyc 13,330 helium pycnometer, Micrometrics Ltd., Dunstable, UK) was very similar between blends, at 0.91–0.93 g/cm^3.

The mixtures were first molten, then transformed into powders by spraying onto a cooled roller, and finally compressed to a compact sample. This process yielded the solid matter under several forms: as a raw material, as a powder, then as a compressed sample.

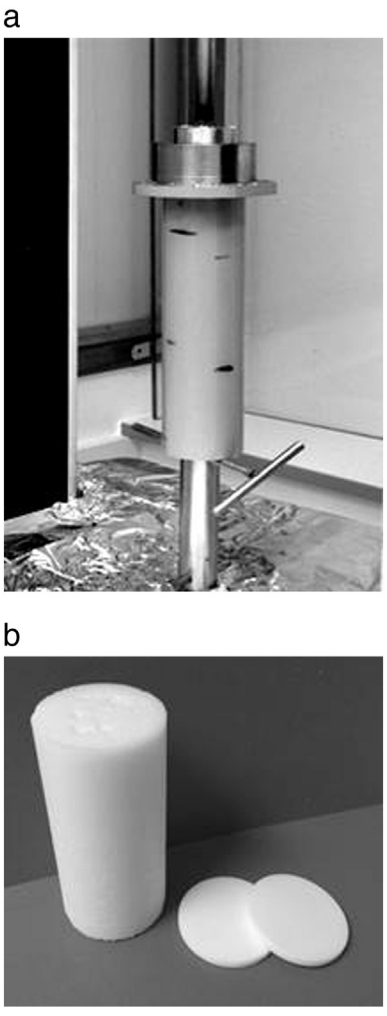

Fig. 4. a) Compression mold to form the sample; b) Compressed sample with Teflon disks used during compression.

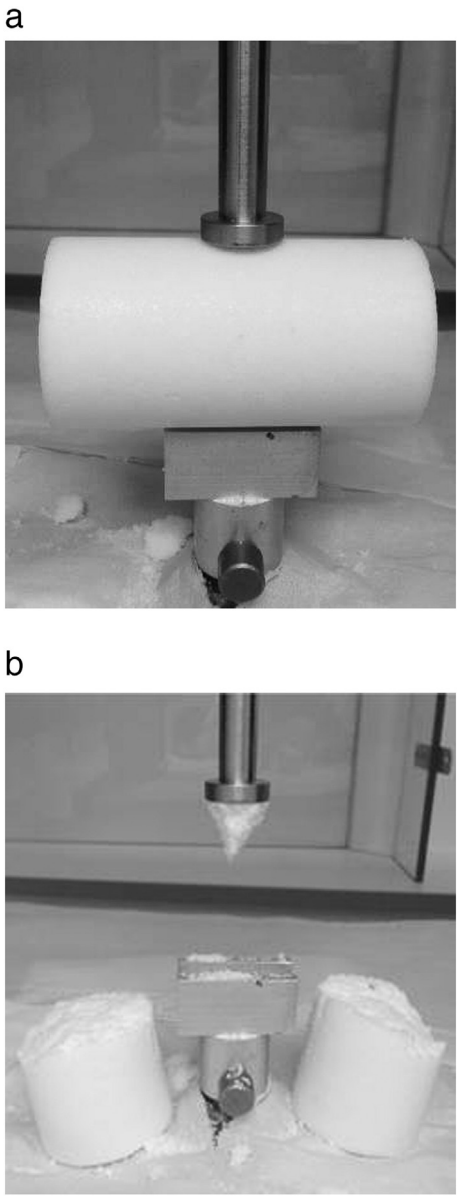

Fig. 5. Principle of the tensile strength measurement of the compressed samples: a) before testing; b) after testing.

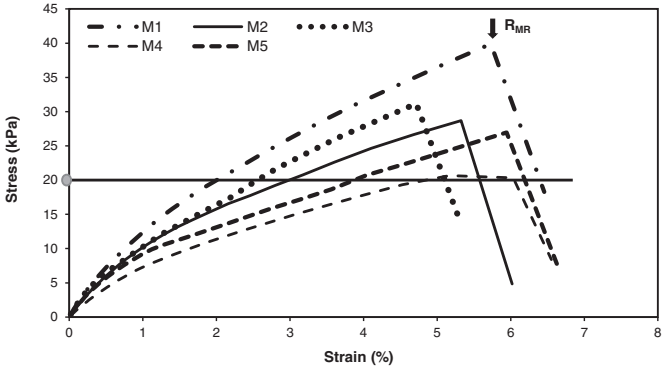

Fig. 6. Stress - strain curves of the five mixtures: –· M1, — M2, ··· M3, – – M4 et — — M5.

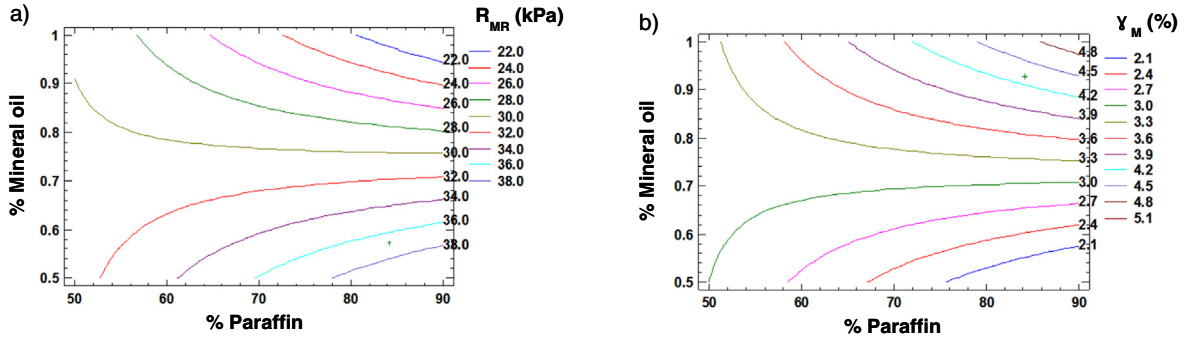

Fig. 7. Iso-response curves: a) stress at rupture, R_{MR}; b) strain at 20 kPa, γ_M, according to the composition in mineral oil and paraffin.

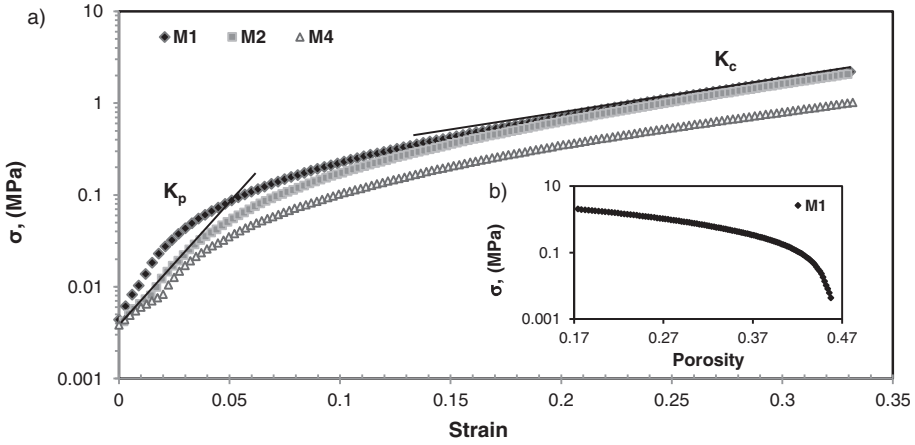

Fig. 8. a) Stress - strain relationship of the compression test at a speed of 10 mm/s, with two coefficients K_p, at low strain range, (0–0.035) and K_c, at higher strain range (0.15–0.33) of the mixtures M1, M2 and M4; b) Evolution of the porosity under stress of the mixture M1.

2.2. Methods

2.2.1. Mechanical properties of the material

In order to determine the properties of the raw materials, the powders were melted, cooled, and cut into rectangular slices of 4 × 65 × 12 mm.

Characterization of the mechanical properties of the material was carried out with a TA Instruments Q800 DMA (Dynamic Mechanical Analysis) instrument (Waters, USA) using the dual cantilever device [23–25]. As illustrated in Fig. 2, in this type of measurement, called 3-point bending, the sample is fixed at both ends and the middle of the sample is also attached to the moving driver. In this mode, the sample is subjected to increasing deformation from 1 μm to 400 μm amplitude in logarithmic mode under oscillating conditions (1 Hz) until rupture. Six replicates were performed for each blend.

As shown in Fig. 3, four characteristics of the material were obtained: Young's modulus, *E*, at low strain (0–0.5%); stress at rupture, R_{MR}; strain at rupture, γ_{MR}; and strain at 20 kPa, γ_M (Fig. 4).

2.2.2. Characterization of the powders

Particle-size distributions were measured by laser diffraction (Malvern MasterSizer 2000, Malvern Instruments, UK) using a dry dispersing unit [16]. Three replicates of each sample were measured. Median diameter D_{50} was determined, and the particle size distribution was characterized by the span, calculated according to Eq. (1):

$$\text{Span} = (D_{90} - D_{10}/D_{50}) \quad (1)$$

Morphology of the individual grains of powder as well as the compressed sample was examined by scanning electron microscopy (SEM, Jeol JSM-7600F, Japan). The samples were deposited on a carbon ribbon and coated with a gold palladium layer for 4 min using a sputtering apparatus (S150 Sputter Coater, Edwards, UK).

2.2.3. Formation of the compressed sample and energy calculations

Uniaxial compression was carried out at laboratory scale to simulate the industrial candle production process and used to evaluate the compressive behavior of the powders and the mechanical properties of the compressed sample [10–12].

The protocol used a texturometer (Lloyd LR5N, Lloyd Instrument Ltd., Southampton, UK) equipped with a 5 kN sensor. An industrial

Table 2
Particle size distribution of the five mixtures ($n = 3$). Mean ± standard deviation.

Mixture	Particle size distribution	
	D_{50} (μm)	Span
M1	1151.9 ± 43.5	1.17 ± 0.03
M2	1121.2 ± 21.7	1.11 ± 0.03
M3	1117.9 ± 47.7	1.18 ± 0.02
M4	1162.5 ± 27.3	1.19 ± 0.03
M5	1448.1 ± 56.9	1.15 ± 0.03

Table 3
Density of the three slices (top, middle and bottom) of the compressed sample for the five mixtures. Mean ± standard deviation. Mean, in column, with the same letter are not significantly different (ANOVA, $p \leq 0.05$, Fisher test).

Mixture	Density of slices (kg/m^3)		
	Top	Middle	Bottom
M1	823.61 ± 0.53 ^{a}	758.95 ± 1.13 ^{a}	711.94 ± 0.79 ^{c}
M2	826.71 ± 0.98 ^{a}	757.84 ± 0.44 ^{a}	728.18 ± 1.94 ^{a}
M3	804.71 ± 2.11 ^{b}	757.48 ± 0.83 ^{a}	721.72 ± 0.70 ^{b}
M4	806.86 ± 1.52 ^{b}	757.28 ± 2.07 ^{a}	722.29 ± 0.56 ^{b}
M5	796.69 ± 0.76 ^{c}	759.06 ± 1.62 ^{a}	721.40 ± 1.28 ^{b}

compression mold of 46 mm internal diameter and 200 mm height was used to mimic industrial candle production conditions. A piston and two Teflon disks were manufactured to prevent the sample sticking to the pistons. A mass of 126 g of powder was introduced into the mold and compressed to the final height of 100 mm at a speed of 10 mm/s. In these conditions, the deformation applied to the powder was fixed at 33%, to reach a final density of 760 ± 2 kg/m^3, which for industrial technology reasons is the optimal density for candle manufacture. Six repetitions were performed for each mixture.

After compression, the samples were weighed (±0.1 mg) and diameter (±0.01 mm) and height (±0.01 mm) were measured by a caliper (DCA150, Velleman, China) to control density.

The heterogeneity in density of the compressed sample [19,28] along the vertical axis was measured by cutting the sample into three 33 mm-thick slices and measuring the density of each slice on a 1000 mL-volume pycnometer (Duran, Schott, Germany). The value reported presented in Table 3 is the mean of three measurements.

Force–displacement data was recorded during the compression. The specific energy, E_s, required to produce the compressed sample was determined according to the methodology of Pampuro et al. [34] and Mani et al. [35]. The area under each curve was integrated using the trapezoidal rule and combined with the powder mass, giving specific energy values in J kg^{-1}. Specific energy values were calculated for 5 mixtures.

2.2.4. Porosity evolution during compression

Porosity, ε, represents the void fraction of a solid material. It is defined as the ratio of the volume of the voids (Vv) to total volume of the material (V_{app}), and can be expressed as [29]:

$$\varepsilon = 1 - \left(\rho_{app}/\rho_s\right) \quad (2)$$

where ε is porosity, ρ_{app} is apparent density of the compressed sample, and ρ_s is the density of the material measured by the AccuPyc 13,330 helium pycnometer (Micrometrics Ltd., Dunstable, UK).

To estimate porosity evolution during compression, ρ_{app} was calculated by Eq. (3):

$$\rho_{app} = m / (h\pi r^2) \quad (3)$$

where m is mass of powder, h is variation of the height of the sample during compression, and r is radius of the sample.

2.2.5. Mechanical properties of the compressed sample

Destructive tests are a mechanical criterion for characterizing the solidity of the sample. The test was performed with the same equipment as for compression (Lloyd LR5N texturometer, Lloyd Instrument Ltd., Southampton, UK) using a 20 mm-diameter piston with a compression speed of 1 mm/s.

The compression was applied radially to the sample until it ruptured, and maximum force was recorded. The tensile strength [37–42] of the compressed sample, σ_t, was calculated from the crushing force (P) according to the equation developed by Hertz [37]:

$$\sigma_t = 2P/\pi dt \quad (4)$$

where P is crushing force (N), d is sample diameter (mm), and t is piston diameter (mm).

As shown in Fig. 5, the tensile strength measurement was carried out on the middle part of the sample [40], on six repetitions.

2.2.6. Statistical analysis

All statistical analyses were performed using XLSTAT statistical data analysis software (Version 2016.5, Addinsoft, New York, USA). Analysis of variance (ANOVA) was used for comparison of experimental data. Multiple comparisons were performed using Fisher's LSD test to analyze the differences between the modalities with a confidence interval of 95%. Principal component analysis (PCA) was used to visualize correlations between mixture variables. All analyses were carried out in six replicates.

3. Results and discussion

3.1. Mechanical behavior of the material

Maximal stress recorded at rupture of the material, R_{MR}, is used to define the mechanical strength of the material (Fig. 6) [22,24]. The mechanical characteristics of the blends are reported in Table 4. Mixture M1 showed the highest stress at rupture (Fig. 6, Table 4). Strain at rupture, γ_{MR}, showed little difference between the five mixtures, whereas strain at 20 kPa stress, γ_M, was clearly different between samples. Mixtures M4 and M5 showed greater deformability (Fig. 6, Table 4).

Young's modulus at low deformations (0–0.5%) characterizes the rigidity of the material in the elastic area [21]. Mixture M1 was stiffer than the other blends, and conversely, mixtures M4 and M5 were softer (Table 4).

Characterizing the mixtures according to their mechanical behavior made it possible to classify them. Mixture M1 showed the behavior of a hard and stiff material with low deformability, whereas mixtures M4 and M5 showed the behavior of a fairly soft material and mixtures M2 and M3 showed a very similar intermediate pattern of mechanical behavior.

The mineral oil and the vegetable oil were found to have an important influence on the mechanical properties of the blends. Fig. 7 and Table 4 show that for the same amount of vegetable oil (15.9%) (Fig. 1 and Table 1), the presence of a higher amount of mineral oil (0.78%) in mixture M4, in contrast to mixture M1 (0.48%), increases the deformability of mixture M4 (γ_M), and logically decreases mechanical stress at rupture (R_{MR}) and stiffness (Young's modulus). The influence of vegetable oil on the mechanical properties of the material also appears important, as shown by mixtures M3 (0.53% mineral oil of the blend and 30% vegetable oil) and M5 (0.52% mineral oil of the blend and 44.1% vegetable oil) that share the same amount of mineral oil whereas M5 is significantly softer than M3.

Table 4
Mechanical characteristics: stress at rupture (R_{MR}), strain at 20 kPa (γ_M), strain at rupture (γ_{MR}) of material and Young's modulus (E). Mean ± standard deviation. Mean, in column, with the same letter are not significantly different (ANOVA, $p \leq 0.05$, Fisher test).

Mixture	Stress at rupture, R_{MR} (kPa)	Strain at 20 kPa, γ_M (%)	Strain at rupture, γ_{MR} (%)	Young's modulus, E (kPa)
M1	35.10 ± 2.15^{a}	2.58 ± 0.15^{d}	5.31 ± 0.34^{b}	14.02 ± 0.46^{a}
M2	30.36 ± 1.13^{b}	3.25 ± 0.21^{c}	$5.65 \pm 0.67^{a,b}$	12.34 ± 0.29^{b}
M3	32.27 ± 0.78^{b}	2.78 ± 0.25^{d}	5.16 ± 0.32^{b}	12.51 ± 0.27^{b}
M4	22.05 ± 1.36^{d}	4.65 ± 0.23^{a}	6.01 ± 0.27^{a}	8.17 ± 0.63^{d}
M5	27.21 ± 1.19^{c}	3.75 ± 0.13^{b}	5.86 ± 0.34^{a}	11.44 ± 0.30^{c}

3.2. Compressive behavior of the powders

Fig. 8a presents the mechanical behavior of the powders based on the uniaxial compression test. Powders of all five mixtures presented a similar particle size distribution of 1.1–1.5 mm (Table 2), but compared to the others, mixture-M5 particles were flake-shaped.

Table 5
Experimental values ($n = 6$) of the K_p coefficient (packing step) and the K_c coefficient (compaction step) of the five mixtures. Mean ± standard deviation. Mean, in column, with the same letter are not significantly different (ANOVA, $p \leq 0.05$, Fisher test).

Mixture	K_p (kPa)	K_c (kPa)
M1	30.98 ± 1.20^{a}	3.72 ± 0.06^{b}
M2	$24.92 \pm 1.29^{b,c}$	4.36 ± 0.04^{a}
M3	27.26 ± 0.80^{b}	3.73 ± 0.04^{b}
M4	23.24 ± 1.56^{c}	3.39 ± 0.08^{b}
M5	18.98 ± 1.76^{d}	4.38 ± 0.09^{a}

The compressive behavior of the powder can be described by the slope of the curve. The curve shows two main regions of strain, i.e. low strain (0–0.035) and high strain (0.15–0.33), and the slope is calculated according to Eq. (5):

$$\log \sigma = a + b \cdot \gamma_c \tag{5}$$

where σ is axial stress applied in compression (Mpa), γ_c is compressive strain, a is the constant, and b and b' are the slopes of the curve at a low and high strain, respectively.

The first region at low strain range (0–0.035) was assimilated to the rearrangement of the particles during compression according to Barbosa-Canovas & Juliano [10] and Järveläinen et al. [11]. The K_p coefficient deduced from slope b in this region represents the resistance to the movement of the particles: the larger the K_p, the lower the compressibility of the powder bed. At low stress (lower than 0.1 MPa), the porosity (Fig. 8b) is larger than the theoretical packing porosity of isodiametric spheres (0.36). This confirms that the volume reduction of the sample is mostly due to the displacement of the particles with relatively small contact deformation [12].

The second region at a high strain range (0.15–0.33) was ascribed to the deformation of the particles during compression. The K_c coefficient, defined as the slope b' of the curve, represents the resistance of the particles during the compaction step. During compaction at large strains, movement between particles is reduced and so they undergo plastic deformation. Such deformations can be observed on Fig. 9b with the appearance of flat surfaces at the contact zones between the spheres. Moreover, bridges at the contact of the particles are observed (Fig. 9c and d) that seem to be different according to composition of the sample [17,27].

As shown in Table 5, mixture M1 showed the highest K_p coefficient and M5 the lowest. The decrease of K_p coefficient, or increase of compressibility, can be explained by a decrease in the resistance of the particles to the friction due to the sliding effect of lubrication played by mineral and vegetable oils [52–53]. The presence of flake particles in mixture M5 is a factor that lowers the resistance of the particles during the packing step [18]. However, it is difficult to dissociate the influence of the powder characteristics from the formulation effect.

Conversely, K_c coefficient varied little between the mixtures analyzed. This could be explained by a greater role of wall friction of the compression cell in that stress region, thus masking any other effect [19–20]. A part of the energy delivered to the piston might be dissipated by wall friction. As shown in Fig. 9, during compression, the particles did not

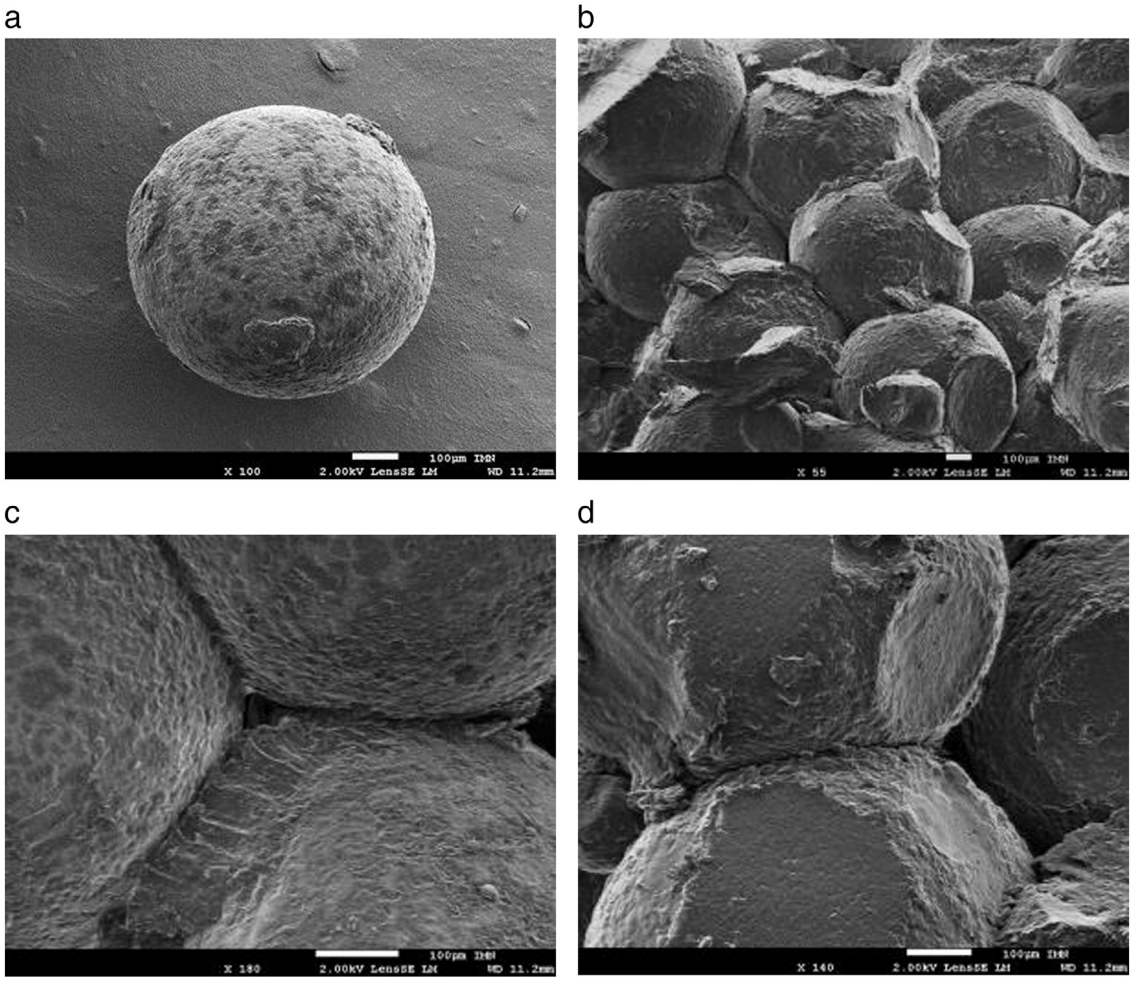

Fig. 9. SEM images of the different samples: a) individual grain of the powder before compression, for mixture M4; b) plastic deformation of the particles after compression, for mixture M4; c) formation of solid bridges between particles, for mixture M1; d) formation of fragile bridges in presence of the mineral oil, for mixture M4.

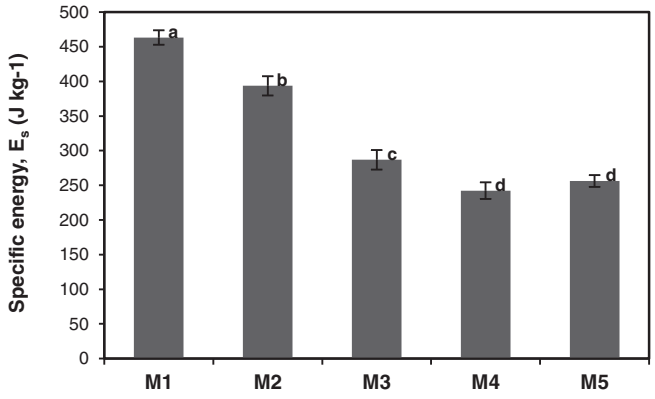

Fig. 10. Specific energy values (J kg^{-1}) required for compression of the five mixtures.

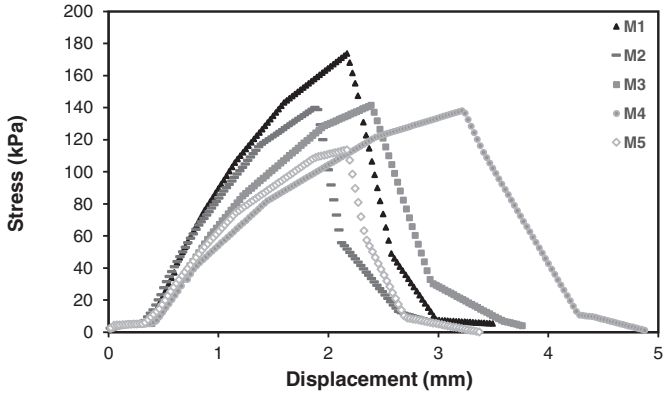

Fig. 12. Stress as a function of the displacement of the piston in the case of the five mixtures: M1, M2, M3, M4 and M5.

fuse but remained individual, due to the low pressure range (1–2 MPa) compared to pressures used in the pharmacy industry (100–200 MPa).

Fig. 10 shows the specific energy required for compression of the powders of the five mixtures. Specific energy evolved in the range 230–470 J kg^{-1} depending on formulation. During compression, mixtures caused different energy absorptions, as shown in the study by Pampuro et al. [34] for two different types of compost. The specific energy values found here for compression of paraffin wax powder were considerably lower than those found by Mani et al. [35] during compaction tests on corn stover where compression used higher pressures (5–15 MPa), giving the briquette density ranging from 650 kg/m^3 to 950 kg/m^3, i.e. close to the densities obtained here (760 kg/m^3). A study by Mani et al. [36] on four biomass species (wheat straw, barley straw, corn stover, switchgrass) reported that energy requirements are dependent on applied pressure and density, and on the nature of the material.

Fig. 11 shows the relationship between the applied stress and the specific energy implemented to form the compressed samples of the five mixtures. The figure shows that specific energy increases with stress applied. Pampuro et al. [34] and Mani et al. [35] reported a similar trend in energy to compact the compost and the corn stover. The M1 and M2 mixtures require more pressure to compress the powder at the same density, and therefore absorb more energy, whereas mixtures M3, M4 and M5 require considerably less energy. It can be concluded that the compression of powder is more efficient when vegetable and mineral oil are present, as specific energy was significantly lower for the same final density of compressed sample for these three mixtures.

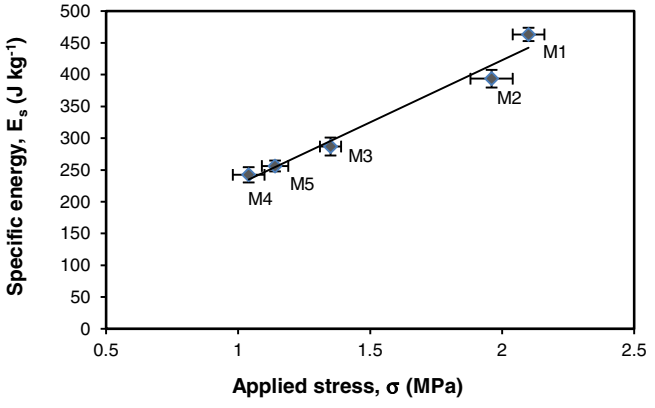

Fig. 11. Relationship between applied stress and specific energy to form the compressed sample for the five mixtures.

3.3. Mechanical properties of compressed samples

The objective of measuring the tensile strength of the compressed samples is to estimate the internal cohesion of the compressed samples and hence their solidity [38,40]. The destructive test is carried out on the middle part of the cylinder where the density is the same for all formulations (Table 3). As shown in Fig. 9c, cohesion of the compacted sample is achieved by the formation of solid bridges between particles, and mechanical breakage of the compressed samples is obtained by their rupture [41].

Fig. 12 shows the evolution of process stress as a function of displacement of the piston for the five mixtures studied. Fig. 13 shows the variation of tensile strength σ_t according to formulation. Statistical processing was able to classify the mixtures into three categories, where mixture M1 exhibits the highest tensile strength, mixtures M2, M3 and M4 show a very similar intermediate behavior, and mixture M5 has the lowest tensile strength.

The mineral and vegetable oils had a significant influence on the mechanical properties of the material and the compressive behavior of the powder. Both components played a lubricating role that reduces the friction between the particles, resulting in a weakening of the bonds and a fragility of the compressed sample. Increased fragility with the presence of lubricant has been observed in the compression of pharmaceutical tablets [57–59], while Yaman et al. [61] found that adding olive refuse had a detrimental effect on the mechanical strength of fuel briquettes.

Particle properties are often referred to as a factor affecting the resistance of compressed powder. The plastic deformation of particles plays an important role in making permanent bonding, as shown in a study by Kaliyan & Morey [50] on the densification of biomass products. The influence of the size and shape of the particles has been widely studied in compression. The study by Pampuro et al. [49] on compression of compost (at 3.5–5 MPa) demonstrated the important influence of 0.5–2 mm-range particle size on briquette strength, with small sizes being preferable to improve the strength of the compacted powder. Here, particle size of the 5 mixes was very similar (1.1–1.5 mm), which certainly weakly influences the result. Furthermore, the flake shape of the particles of mixture M5 seems to make the compressed samples easier to crack and fracture, as also shown by Nikolakakis & Pilpel [43] and Kaliyan & Morey [50].

Kaliyan & Morey [50] studied several factors affecting the strength of densified biomass products, and found that mechanical strength increases with density of the compacts and the specific energy required during compression. The specific energy required to obtain the same volume is lower for powders, which are then more compressible [14,54], and the combination of mineral oil and vegetable oil strongly reduces the mechanical strength of the candles (in the case of mixture

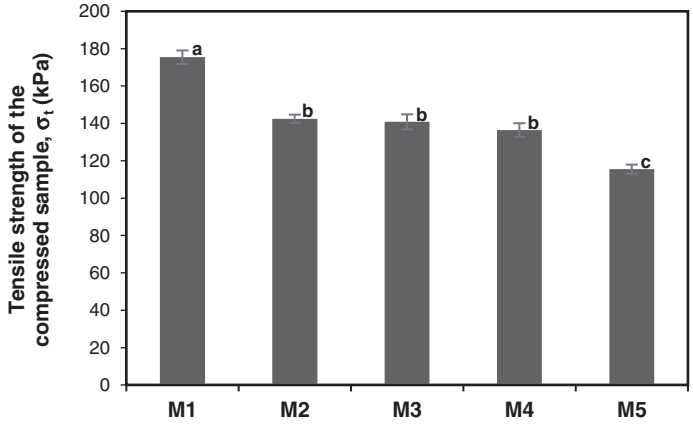

Fig. 13. Tensile strength of the compressed sample σ_t for the five mixtures: M1, M2, M3, M4 and M5.

M5), which limits the use of the mineral oil and vegetable substitutes in the manufacture of candles by compression.

3.4. Influence of overall mechanical characteristics on tensile strength of the compressed samples

Fig. 14 presents the PCA used to visualize correlations between variables. The mechanical parameters of the material and of the compressive behavior of the powders as well as the formulation are taken into account to explain the tensile strength of the compressed samples. The first axis describes the properties of the material: strain at 20 kPa is situated opposite stress at rupture and Young's modulus. The second vertical axis corresponds to formulation.

Analysis of the mechanical parameters of the material studied in DMA found that strain at 20 kPa (γ_M), stress at rupture (R_{MR}) and Young's modulus (E) can be related to the tensile strength of the compressed samples (σ_t). According to Fig. 14, material deformability (γ_M) is unfavorable to the solidity of the compressed samples as represented by tensile strength—indeed, the mechanical strength (R_{MR}) and stiffness (E) of the material on the contrary promote a fairly high tensile strength of the compressed samples.

The compressive behavior of the powders also influences the tensile strength of the compressed samples. K_p coefficient represents the resistance of the particles to rearrangement during the packing step to form a compact medium. K_p coefficient is the characteristic that most closely correlates to the tensile strength of the compressed samples, and increases with it. This means that higher resistance to deformation in the packing step is correlated to solidity of the compressed sample. The specific energy required to compress the powder is also related to the tensile strength of compressed samples, as it increases with resistance of the compressed samples.

The formulation that promotes high tensile strength of the compressed samples (M1) is characterized by low deformability (γ_M) with both high mechanical strength (R_{MR}) and high Young's modulus of the material. The material that enhances the tensile strength of the compressed samples is characterized by high particle resistance to rearrangement (K_p) and high specific energy of the powder during compression. High mineral oil content (M4) decreases the hardness of the material and facilitates the compressibility of the powders. Moreover, it has a strong and negative influence on the tensile strength of the compressed samples, as it acts as a lubricant. The presence of vegetable oil reduces particle resistance to rearrangement, thereby reducing the tensile strength of the compressed samples.

To summarize, tensile strength of the compressed samples is strongly influenced by the formulation, and especially by the presence of lubricant in the material. Mineral and vegetable oil decrease resistance to compression (K_p), and likely also the strength of the bridges between particles during compaction, thus decreasing the tensile strength of the compressed samples.

4. Conclusion

The influence of the mechanical characteristics of the material and compressive behavior of the powder on the tensile strength of the compressed sample was studied. The K_p coefficient representing particle resistance to rearrangement during the packing step is the parameter most correlated with tensile strength of the compressed samples, and increases with it. Specific energy in compression also increases with strength of the compressed sample. The mechanical properties of the material analyzed in DMA are further characteristics that help explain the tensile strength of the compressed sample. High-tensile-strength samples come from mixtures with low deformation capacity and with hard material characterized by a high Young's modulus. The presence

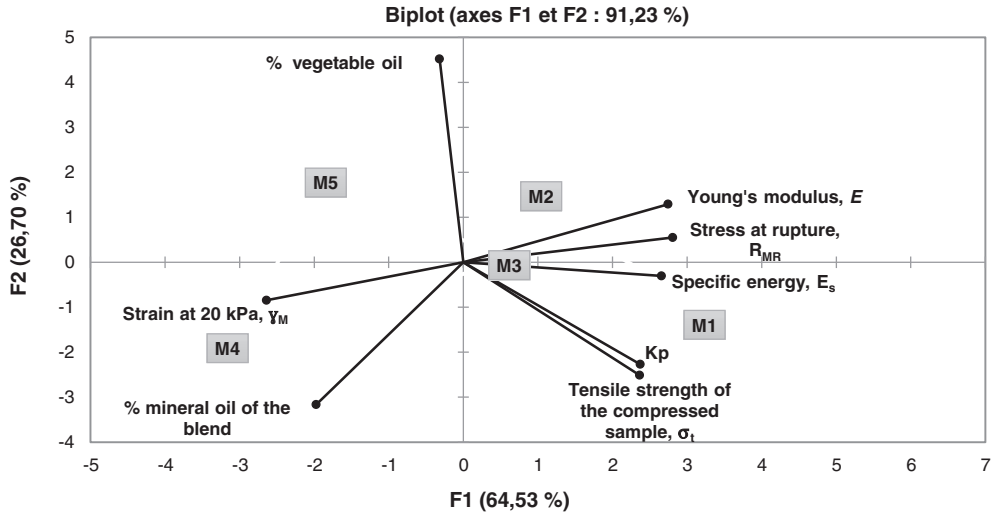

Fig. 14. PCA according to the mechanical parameters of the material: strain at 20 kPa (γ_M), stress at rupture (R_{MR}) and Young's modulus (E); K_p coefficient and specific energy (E_s); formulation components: % mineral oil of the blend and % vegetable oil; and tensile strength of the compressed sample (σ_t) for the five mixtures M1, M2, M3, M4 et M5.

of mineral oil and vegetable substitute both play a lubricant role and have a huge influence on the mechanical properties of both the material and the compressed sample. The specific energy required for powder densification decreases in presence of the two oils, which makes it possible to reduce energy expenditure in compression but impossible to obtain sufficiently strong compressed samples.

The paraffin, which is assimilated to a hard material with a lower capacity to be deformed at a low percentage of mineral oil, showed the highest tensile strength of the compressed samples. However, it is difficult to substitute paraffin by vegetable oil at 44.1%, as the incorporation facilitates the compression of the powder but weakens the tensile strength of the compressed sample. A higher percentage of substitution might be considered if the compression can be conducted at higher stresses and hence densities, as it would reinforce the cohesive forces between the grains and therefore enhance the tensile strength of the compressed sample. Clearly, there is a trade-off to be found between the acceptable level of strength of the candles and the limit of incorporation of the vegetable substitute.

Acknowledgements

The authors thank Christophe Couedel for his valuable technical assistance.

References

[1] T.A. Murphy, Triacyglycerol-based wax for use in container candlesPatent number US6797020 B2 2004.
[2] T.A. Murphy, M.K. Doucette, N.C. House, M.L. Richards, Triacyglycerol-based alternative to paraffin waxPatent number US8202329 B2 2012.
[3] B. Tao, A. Hutchison, Vegetable lipid-based composition and candlePatent number US8404003 B2 2013.
[4] Y. Victory, H. Koji, O. Fumiko, A. Shuji, M. Masakicho, CandlePatent number JP3149509U 2009.
[5] P. York, Crystal engineering and particle design for the powder compaction process, Drug Dev. Ind. Pharm. 18 (1992) 677–721.
[6] C. Sun, D.J. Grant, Influence of crystal shape on the tableting performance of L-lysine monohydrochloride dehydrate, J. Pharm. Sci. 90 (2001) 569–579.
[7] R.W. Heckel, Density–pressure relationships in powder compaction, Trans. Metall. Soc. AIME 221 (1961) 671–675.
[8] R.W. Heckel, An analysis of powder compaction phenomena, Trans. Metall. Soc. AIME 221 (1961) 1001–1008.
[9] K. Kawakita, K.H. Ludde, Some considerations on powder compression equations, Powder Technol. 4 (1970/71) 61–68.
[10] G.V. Barbosa-Canovas, P. Juliano, Compression and compaction characteristics of selected food powders, Adv. Food Nutr. Res. 49 (2005) 233–307.
[11] M. Järveläinen, A. Kaleva, A. Kaitajärvi, J. Laakso, U. Kanerva, E. Levänen, Compression curve analysis and compressive strength measurement of brittle granule beds in lieu of individual granule measurements, J, Particuology 29 (2016) 60–68.
[12] M. Stasiak, J. Tomas, M. Molenda, R. Rusinek, P. Mueller, Uniaxial compaction behavior and elasticity of cohesive powders, Powder Technol. 203 (2010) 482–488.
[13] K. Marshall, Compression and Consolidation of Powdered Solids, in: L. Lachman, H.A. Lieberman, J.L. Kanig (Eds.), The Theory and Practice of Industrial Pharmacy, 3rd edVarghese Publishing, Bombay, 1987.
[14] V. Jannin, V. Bérard, S. Chevrier, A. Malmazet, Y. Chavant, F. Demarne, C. Andrès, Functional characterization of powders consisting of mixtures of glyceryl behenate and a non-ionic surfactant applied by hot-melt coating: lubricant performance, J. Drug Del. Sci. Tech. 23 (2) (2013) 181–185.
[15] H.M. MacLeod, Compaction of Ceramics, in: N.G. Stanley-Wood (Ed.), Enlargement and Compaction of Particulate Solids, 259, Butterworths, London 1983, p. 39.
[16] L. Qu, P.J. Stewart, K.P. Hapgood, K. Lakio, D.A.V. Morton, Q. Zhou, Single-step coprocessing of cohesive powder via mechanical dry coating for direct tablet compression, J. Pharm. Sci. 106 (1) (2016) 159–167.
[17] C. Nystrom, G. Alderborn, M. Duberg, P.G. Karehill, Bonding surface area and bonding mechanism – two important factors for the understanding of powder compactibility, Drug Dev. Ind. Pharm. 19 (1993) 2143–2196.
[18] H.A. Garekani, J.L. Ford, M.H. Rubinstein, A.R. Rajabi-Siahboomi, Effect of compression force, compression speed and particle size on the compression properties of paracetamol, Drug Dev. Ind. Pharm. 27 (2001) 935–942.
[19] C.-Y. Wu, O.M. Ruddy, A.C. Bentha, B.C. Hancock, S.M. Best, J.A. Elliott, Modelling the mechanical behaviour of pharmaceutical powders during compaction, Powder Technol. 152 (2005) 107–117.
[20] B.J. Briscoe, S.L. Rough, The effects of wall friction in powder compaction, Colloids Surf. A. Physicochem. Eng. Asp. 137 (1998) 103–116.
[21] R.J. Roberts, R.C. Rowe, The Young's modulus of pharmaceutical materials, Int. J. Pharm. 37 (1987) 15–18.
[22] M.J.M. Ridzuan, M.S. Abdul Majid, M. Afendi, M.N. Mazlee, A.G. Gibson, Thermal behavior and dynamic mechanical analysis of *Pennisetum purpureum*/glass-reinforced epoxy hybrid composites, Compos. Struct. 152 (2016) 850–859.
[23] N. Saba, M.T. Paridah, K. Abdan, N.A. Ibrahim, Dynamic mechanical properties of oil palm nano filler/kenaf/epoxy hybrid nanocomposites, Constr. Build. Mater. 124 (2016) 133–138.
[24] A. Jabbar, J. Militky, J. Wiener, B.M. Kale, U. Ali, S. Rwawiire, Nanocellulose coated woven jute/green epoxy composites: characterization of mechanical and dynamic mechanical behavior, Compos. Struct. 161 (2017) 340–349.
[25] S.E. Zeltmann, B. Kumar, M. Doddamani, N. Gupta, Prediction of strain rate sensitivity of high density polyethylene using integral transform of dynamic mechanical analysis data, Polymer 101 (2016) 1–6.
[26] K.V. Pillai, S. Renneckar, Dynamic mechanical analysis of layer-by-layer cellulose nanocomposites, Ind. Crop. Prod. 93 (2016) 267–275.
[27] G. Alderborn, C. Nystrom (Eds.), Pharmaceutical Powder Compaction Technology, Marcel Dekker Inc., New York, 1996.
[28] A. Michrafy, D. Ringenbacher, P. Techoreloff, Modelling the compaction behavior of powders: application to pharmaceutical powders, Powder Technol. 127 (2002) 257–266.
[29] V. Kumar, D. Reus-Medina, D. Yang, Preparation, characterization and tableting properties of a new cellulose-based pharmaceutical aid, Int. J. Pharm. 235 (1–2) (2002) 129–140.
[30] E.N. Hiestand, J.E. Wells, C.B. Peot, J.F. Ochs, Physical processes of tableting, J. Pharm. Sci. 66 (1977) 510–519.
[31] S.T. David, L.L. Augsburger, Plastic flow during compression of directly compressible fillers and its effect on tablet strength, J. Pharm. Sci. 66 (1977) 155–159.
[32] F. Podczeck, The determination of fracture mechanics properties of pharmaceutical materials in mode III loading using an anti-clastic plate bending method, Int. J. Pharm. 227 (2001) 39–46.
[33] M. Celik, Compaction of Multiparticulate Oral Dosage Forms, in: I. Ghebre-Sellassie (Ed.), Multiparticulate Oral Drug Delivery, Marcel Dekker, New York, 1994.
[34] N. Pampuro, A. Facello, E. Cavallo, Pressure and specific energy requirements for densification of compost derived from swine solid fraction, Span. J. Agric. Res. 11 (2013) 678–684.
[35] S. Mani, L.G. Tabil, S. Sokhansanj, Specific energy requirement for compacting corn stover, Bioresour. Technol. 30 (2006) 648–654.
[36] S. Mani, L.G. Tabil, S. Sokhansanj, Evaluation of compaction equations applied to four biomass species, Can. Biosyst. Eng. 46 (2004) 351–361.
[37] S.P. Timoshenko, J.N. Goodier, Theory of Elasticity, McGraw Hill, New York, 1970.
[38] P. Stanley, Mechanical strength testing of compacted powders, Int. J. Pharm. 227 (2001) 27–38.
[39] J.T. Fell, J.M. Newton, Determination of tablet strength by the diametral-compression test, J. Pharm. Sci. 59 (1970) 688–691.
[40] L. Castrati, V. Mazelb, V. Busigniesb, H. Diarrab, A. Rossia, P. Colomboa, P. Tchoreloff, Comparison of breaking tests for the characterization of the interfacial strength of bilayer tablets, Int. J. Pharm. 513 (2016) 709–716.
[41] C. Shang, I.C. Sinka, B. Jayaraman, J. Pan, Break force and tensile strength relationships for curved faced tablets subject to diametrical compression, Int. J. Pharm. 442 (2013) 57–64.
[42] M.C. Shaw, P.M. Braiden, G.J. Desalvo, The disk test for brittle materials, ASME J. Eng. Ind. (1975) 77–87.
[43] I. Nikolakakis, N. Pilpel, Effect of particle size and particle shape on the tensile strengths of powders, Powder Technol. 45 (1) (2001) 79–82.
[44] G. Alderborn, E. Borjesson, M. Glazer, C. Nystrom, Studies on direct compression of tablets. XIX the effect of particle size and shape on the mechanical strength of sodium bicarbonate tablets, Acta Pharm. Suec. 25 (1988) 31–40.
[45] E. Ryshkewitch, Compression strength of porous sintered alumina and zirconia, J. Am. Ceram. Soc. 3 (2) (1953) 65–68.
[46] B.V. Veen, K.V.D. Maarschalk, G.K. Bolhuis, K. Zuurman, H.W. Frijlink, Tensile strength of tablets containing two materials with a different compaction behavior, Int. J. Pharm. 203 (1–2) (2000) 71–79.
[47] T. Sebhatu, G. Alderborn, Relationships between the effective interparticulate contact area and the tensile strength of tablets of amorphous and crystalline lactose of varying particle size, Eur. J. Pharm. Sci. 8 (1999) 235–242.
[48] M.C.I. Amin, J.T. Fell, Tensile strength and bonding in compacts: a comparison of diametral compression and three-point bending for plastically deforming materials, Drug Dev. Ind. Pharm. 28 (7) (2002) 809–813.
[49] N. Pampuro, G. Bagagiolo, P.C. Priarone, E. Cavallo, Effects of pelletizing pressure and the addition of woody bulking agents on the physical and mechanical properties of pellets made from composted pig solid fraction, Powder Technol. 311 (2017) 112–119.
[50] N. Kaliyan, R.V. Morey, Factors affecting strength and durability of densified biomass products, Biomass Bioenergy 33 (2009) 337–359.
[51] T.A. Miller, P. York, Pharmaceutical tablet lubrication, Int. J. Pharm. 41 (1988) 1–19.
[52] J. Wang, H. Wen, D. Desai, Lubrication in tablet formulations, Eur. J. Pharm. Biopharm. 75 (2010) 1–15.
[53] M.O. Bastos, R.B. Friedrich, R.C.R. Beck, Effects of filler-binders and lubricants on physicochemical properties of tablets obtained by direct compression: a 2^2 factorial design, Lat. Am. J. Pharm. 27 (4) (2008) 578–583.
[54] Y. Li, H. Liu, A. Rockabrand, Wall friction and lubrication during compaction of coal logs, Powder Technol. 87 (1996) 259–267.
[55] J. Li, Y. Wu, Lubricants in pharmaceutical solid dosage forms, Lubricants 2 (1) (2014) 21–43.
[56] G.K. Bolhuis, S.W. De Jong, H.V. Van Kamp, H. Dettmers, The effect on tablet crushing strength of magnesium stearate admixing in different types of lab-scale and production-scale mixers, Pharm. Tech. Jpn. 3 (1987) 877–883.

[57] P.J. Jarosz, E.L. Parrott, Effect of lubricant on tensile strengths of tablets, Drug Dev. Ind. Pharm. 10 (1984) 2059–2073.
[58] X.R. He, P.J. Secreast, G.E. Amidon, Mechanistic study of the effect of roller compaction and lubrication on tablet mechanical strength, J. Pharm. Sci. 96 (2007) 1342–1355.
[59] S. Yu, M. Adams, B. Gururajan, G. Reynolds, R. Roberts, C.Y. Wu, The effect of lubrication on roll compaction, ribbon milling, and tableting, Chem. Eng. Sci. 86 (2013) 9–18.
[60] A.M. Miguélez-Morán, C.Y. Wu, J.P.K. Seville, The effect of lubrication on density distribution of roller compacted ribbons, Int. J. Pharm. 362 (2008) 52–59.
[61] S. Yaman, M. Sahan, H. Haykiri-Acma, K. Sesen, Fuel briquettes from biomass-lignite blends, Fuel Process. Technol. 72 (2001) 1–8.